Functional analysis of Lsm protein under multiple stress conditions in the extreme haloarchaeon *Haloferax mediterranei*

Gloria Payá, Vanesa Bautista, Mónica Camacho, María-José Bonete[*], Julia Esclapez

Agrochemistry and Biochemistry Department, Biochemistry and Molecular Biology Area, Faculty of Science, University of Alicante, Ap 99, 03080, Alicante, Spain

ARTICLE INFO

ABSTRACT

The Sm, like-Sm, and Hfq proteins belonging to the Sm superfamily of proteins are represented in all domains of life. These proteins are involved in several RNA metabolism pathways. The functions of bacterial Hfq and eukaryotic Sm proteins have been described, but knowledge about the *in vivo* functions of archaeal Sm proteins remains limited. This study aims to improve the understanding of Lsm proteins and their role using the haloarchaeon *Haloferax mediterranei* as a model microorganism. The *Haloferax mediterranei* genome contains one *lsm* gene that overlaps with the *rpl37e* gene. To determine the expression of *lsm* and *rpl37e* genes and the co-transcription of both, reverse transcription-polymerase chain reaction (RT-PCR) analyses were performed under different standard and stress conditions. The results suggest that the expression of *lsm* and *rpl37e* is constitutive. Co-transcription occurs at suboptimal salt concentrations and temperatures, depending on the growth phase. The halophilic Lsm protein contains two Sm motifs, Sm1 and Sm2, and the sequence encoding the Sm2 motif also constitutes the promoter of the *rpl37e* gene. To investigate their biological functions, the lsm deletion mutant and the Sm1 motif deletion mutant, where the Sm2 motif remained intact, were generated and characterised. Comparison of the *lsm* deletion mutant, Sm1 deletion mutant, and the parental strain HM26 under standard and stress growth conditions revealed growth differences. Finally, swarming assays in complex and defined media showed greater swarming capacity in the deletion mutants.

© 2021 Elsevier B.V. and Société Française de Biochimie et Biologie Moléculaire (SFBBM). All rights reserved.

1. Introduction

The Sm protein superfamily includes Sm, like-Sm (Lsm), and Hfq proteins, all of which are involved in RNA metabolism [1—3]. The Sm and Lsm proteins are found in *Archaea* and *Eukarya* domains, whereas Hfq proteins exist in the *Bacteria* domain and one archaeon species, *Methanocaldococcus jannaschii* [2—5]. The Lsm and Hfq proteins present important differences at the amino acid sequence level; however, they share a bipartite signature sequence known as the Sm domain. This domain consists of two segments, the Sm1 and Sm2 motifs, separated by a region of variable length and amino acid sequence [6]. Although the Lsm and Hfq proteins are not very similar at the primary structure level, they show striking similarities in their tertiary and quaternary structure levels [3,6,7]. The bacterial Hfq proteins form stable hexamers that bind preferentially to A-U rich sequences [8], while the eukaryotic Lsm proteins form five different hetero-heptameric complexes. In contrast, archaeal Lsm protein structures are composed of hexameric [9] or heptameric complexes [10—13]. Moreover, the Lsm protein of *Haloferax volcanii* forms homoheptameric complexes *in vitro* [14]. These observations suggest that Hfq may represent an ancient, less-specialised form of the Sm family of proteins [15].

The eukaryotic Sm proteins constitute the cores of the uracil-rich small nuclear RNPs (U snRNPs) that further assemble into spliceosomes and excise introns in eukaryotic pre-mRNAs [16]. Numerous studies have shown that eukaryotic Sm proteins function as molecular scaffolds for RNP assembly and are involved in mRNA degradation, mRNA decapping, RNA stabilisation, mRNA splicing, telomere maintenance, and histone maturation [6]. The archaeal Lsm proteins were discovered by database sequence search [17]. These proteins were not necessarily expected in

archaea because of the absence of introns in their protein-coding genes and their primitive RNA-processing machinery [15]. However, crystallographic studies [11−13] proved that the architecture of the Sm core domain and RNA binding site was conserved in these archaeal and eukaryotic proteins, including an Sm-like (Lsm) subfamily. In addition, over 50 years ago, the Hfq protein was mentioned for its role in the replication of the RNA phage Qβ [18−20]; however, it is currently known to have a multitude of cellular functions [7]. For example, one of the identified roles of Hfq corresponds to its interaction with sRNAs that regulate gene expression, cooperating as an RNA chaperone with small regulatory RNAs and their target mRNAs, facilitating their connections [21]. The *hfq* insertion mutant in *E. coli* exhibited pleiotropic phenotypes affecting growth rate, cell morphology, and tolerance to stress conditions [22]. These abnormal phenotypes might be produced because Hfq is required for the regulatory function of sRNAs [23−25]. The bacterial homolog Hfq has been widely studied in several bacterial species by generating *hfq* deletion mutants. This protein is involved in the regulation of different stress conditions, such as heat shock, oxidative stress, osmotic stress, UV exposure, acid pH, and ethanol stress [22,26−30]. Moreover, Hfq plays an essential role in pathogenic bacterial motility and virulence [31,32]. However, the functions of archaeal Lsm proteins under stress conditions have not been reported.

Little is known about the physiological functions of archaeal Lsm proteins, although various protein structures have been solved [9,11−13]. The crustal structures of Lsm proteins from *Archaeoglobus fulgidus* and *Pyrococcus abyssi* revealed that the proteins bind to U-rich RNA similar to eukaryotic Lsm and Hfq [13,33]. Moreover, the Lsm proteins from *A. fulgidus* interact with each other and RNase P RNA, similar to eukaryotic Lsm [13]. Further studies highlighted that archaeal Lsm binds with several sRNAs, which suggests a similar function in the sRNA regulatory network as bacterial Hfq protein [14,34]. Additionally, Lsm1 and Lsm2 of *Sulfolobus solfataricus* cooperate with the archaeal exosome proteins for mRNA degradation [35]. Other biological functions have been described in *H. volcanii* where Lsm1 binds with sRNAs that interact with proteins related to translation, stress, nucleic acid metabolism, and the cell cycle, indicating that Lsm is involved in many cellular processes [14]. Therefore, it is unknown whether archaeal Lsm proteins act as chaperones for small regulatory RNAs, as in bacteria, or act as scaffolds, as in eukaryotes [15]. The *lsm* gene of *H. volcanii* was co-transcribed with the overlapping gene of the ribosomal protein L37e, generating a bicistronic transcript and a smaller transcript from the gene for L37e protein under aerobic growth in 2.1 M NaCl at 42 °C, 2.1 M NaCl at 48 °C, and 1.5 M NaCl at 42 °C, while no transcripts were detected under aerobic growth in 2.1 M NaCl at 30 °C and anaerobic growth in 2.1 M NaCl at 42 °C [14]. The Sm2 motif of the *H. volcanii lsm* gene contains a promoter that regulates the expression of the overlapping *rpl37R* gene [36]. Notably, only a bicistronic mRNA of *lsm* and *rpl37R* was detected [14,36]. In addition, the *lsm* deletion mutant was viable in *H. volcanii*, and its phenotype is manifested only in different carbon sources [14]. Moreover, a deletion mutant of the Sm1 motif versus parental strain showed differences in the transcriptome in rich medium (Hv-YPC); the deletion mutant exhibited gain-of-function swarming activity compared to the parental strain [36].

H. mediterranei (isolated from solar salterns, Spain) [37] and *Hfx. volcanii* (isolated from the Dead Sea) [38] are different species of the class Halobacteria. The 16S rRNA sequences of these two species share 98.4% similarity, which implies a divergence time of approximately 80 million years [39]. Notably, these species present numerous differences: (1) *H. mediterranei* is highly vacuolated, whereas *H. volcanii* is not; (2) *H. mediterranei* presents slightly motile during the exponential phase, whereas *H. volcanii* is non-motile; (3) the cell wall of *H. mediterranei* has an entirely different ultrastructural appearance than Halobacterium species; (4) the cell envelopes of *H. mediterranei* are deprived of peptidoglycan; (5) the bulk composition of acids over basics amino acids is higher (19.9% mole excess) than the bulk amino acid composition of *H. volcanii* (15.1% mole excess); (6) the G+C content of DNA (60 mol %) is lower than other Halobacterium species; (7) *H. mediterranei* requires 0.02 M of Mg^{++} for growth, while *H. volcanii* requires 0.08 M; (8) at low salt concentrations, lysis of cells occurs in Halobacterium species; however, *H. mediterranei* cells can survive at low salt concentrations; (9) *H. mediterranei* can hydrolyse starch, gelatine, and Tween, whereas *H. volcanii* does not; (10) *H. mediterranei* cannot produce H_2S from thiosulfate (halobacterial feature); (11) *H. mediterranei* performs complete denitrification, whereas *H. volcanii* cannot produce N_2 from NO_3^-; (12) *H. mediterranei* produces exopolysaccharides; and, (13) *H. mediterranei* is extremely halophilic with optimal growth at 2.9 M NaCl at 40 °C, while *H. volcanii* requires 1.7−2.5 M NaCl and a temperature of 30−40 °C for optimum growth [37,38].

Recently, we identified the sRNAs of *Haloferax mediterranei* according to the nitrogen source [40,41]. *H. mediterranei* contains one gene encoding the Lsm1 protein (HFX_RS09865) in its genome, which shares 99% sequence identity with the Lsm protein of *H. volcanii*. These results suggest that the interaction between Lsm proteins and sRNAs and their participation in RNA metabolism might also occur in *H. mediterranei*. Moreover, Lsm protein is often encoded adjacent to or overlapping with the *rpl37e* gene [15]. The Sm2 motif of the *lsm* gene in *H. volcanii* contains a promoter that regulates the expression of the overlapping *rpl37R* gene, which is wholly preserved in *H. mediterranei*.

The present study presents an extensive analysis of the *lsm* gene from the extreme haloarchaeon *H. mediterranei* under several different conditions, including various nitrogen sources and stress conditions. For this purpose, the transcriptional expression analysis of *lsm* and *rpl37e* genes and their co-transcription were performed under different standard and stress conditions and verified by reverse transcription-polymerase chain reaction (RT-PCR) in the parental strain. Deletion mutants of the open reading frame of the *lsm* gene and the Sm1 motif maintaining the intact specific *rpl37e* promoter were generated and extensively characterised under the same conditions to investigate the metabolic processes in which the Lsm protein plays an essential role.

2. Materials and methods

2.1. Strains, vectors, and standard conditions

Haloferax mediterranei strains R4 (ATCC 33500[T]) [42], HM26 (R4 Δ*pyrE2*) [43], HM26-Δ*lsm* (R4 Δ*pyrE2* Δ*lsm1*), and HM26-ΔSm1 (R4 Δ*pyrE2* ΔSm1) were employed and/or generated in this study. The pMH101 N vector [43] was used to create deletion mutants (HM26-Lsm and HM26-Sm1). The standard conditions for *H. mediterranei* were defined as the growth conditions with aeration at 180 rpm at 42 °C, containing a 25% (*w/v*) mixture of inorganic salts in the complex medium [44] (Table 1).

2.2. Culture media and growth conditions

H. mediterranei was grown in different culture media under different growth conditions (Table 1). The pH of all media was adjusted to 7.2−7.4, with NaOH. Cell samples were collected in the mid-exponential and stationary phases of each culture medium. To study the effect of nitrogen and carbon starvation, *H. mediterranei* cells were grown in 40 mM NH$_4$Cl and 10 g/L glucose medium until the mid-exponential phase. Subsequently, cells were harvested by

Table 1
Culture media and growth conditions.

Study variable	Culture media type	Culture media composition	Salt water (%)	Temperature
Temperature	Complex medium (standard condition)	0.5% (w/v) yeast extract and 100 mM MOPS	25%	**42 °C**
	Complex medium	0.5% (w/v) yeast extract and 100 mM MOPS	25%	**32 °C**
	Complex medium	0.5% (w/v) yeast extract and 100 mM MOPS	25%	**52 °C**
Salinity	Complex medium	0.5% (w/v) yeast extract and 100 mM MOPS	**18%**	42 °C
	Complex medium	0.5% (w/v) yeast extract and 100 mM MOPS	**30%**	42 °C
Oxidative stress	Complex medium	0.5% (w/v) yeast extract, 100 mM MOPS and **2 mM H$_2$O$_2$**	25%	42 °C
Ethanol stress	Complex medium	0.5% (w/v) yeast extract, 100 mM MOPS and **1% (v/v) ethanol**	25%	42 °C
Nitrogen source	Defined medium	**40 mM NH$_4$Cl** and 10 g/L glucose 0.0005 g/L FeCl$_3$, 0.5 g/L KH$_2$PO$_4$, 100 mM MOPS, and 50 µg/mL uracil	25%	42 °C
	Defined medium	**40 mM KNO$_3$** and 10 g/L glucose 0.0005 g/L FeCl$_3$, 0.5 g/L KH$_2$PO$_4$, 100 mM MOPS, and 50 µg/mL uracil	25%	42 °C
Nitrogen source and carbon starvation	Defined medium	**40 mM NH$_4$Cl** 0.0005 g/L FeCl$_3$, 0.5 g/L KH$_2$PO$_4$, 100 mM MOPS, and 50 µg/mL uracil	25%	42 °C
	Defined medium	**40 mM KNO$_3$** 0.0005 g/L FeCl$_3$, 0.5 g/L KH$_2$PO$_4$, 100 mM MOPS, and 50 µg/mL uracil	25%	42 °C
Nitrogen starvation	Defined medium	**10 g/L glucose** 0.0005 g/L FeCl$_3$, 0.5 g/L KH$_2$PO$_4$, 100 mM MOPS, and 50 µg/mL uracil	25%	42 °C

centrifugation for 10 min at 13000×*g*, washed twice with 25% salt water (SW), and transferred to a medium in the absence of nitrogen or carbon source. The *H. mediterranei* cells were subjected to nitrogen or carbon starvation for 48, 96, and 120 h.

2.3. RNA isolation

The *H. mediterranei* cells were lysed with RNAse-free water, and RNA was isolated using TRIzol™ Reagent (Ambion, Thermo Fisher Scientific, Waltham, MA, USA) following the manufacturer's instructions. The concentration and quality of RNA samples were quantified by absorbance using the NanoDrop™ Spectrophotometer (Thermo Fisher Scientific, Waltham, MA, USA).

2.4. Reverse transcription-polymerase chain reaction

The expression of *lsm* (HFX_RS09865) and *rpl37e* (HFX_RS09870) genes and their co-transcription were analysed by RT-PCR. RNA was isolated as described previously. Afterwards, the RNA samples were treated with Turbo DNase (Ambion, Thermo Fisher Scientific, Waltham, MA, USA) following the manufacturer's instructions. DNA-free RNA (0.8 µg) was used for the synthesis of cDNA using *M-MuLV* Reverse Transcriptase (Thermo Fisher Scientific, Waltham, MA, USA) and random hexamer primers (Thermo Fisher Scientific, Waltham, MA, USA) according to the manufacturer's instructions. Negative controls for RT-PCR were prepared by omitting the reverse transcriptase or cDNA. The primers used for RT-PCR were LsmF/LsmR for *lsm* expression, Rpl37eF/Rpl37eR for *rpl37e* expression, and LsmF/Rpl37eR for the co-transcription of both genes (Supplementary Table 1). PCR products were analysed using 1.6% (w/v) agarose gel electrophoresis with a GeneRuler™ Range DNA Ladder (Thermo Fisher Scientific, Waltham, MA, USA) run in parallel.

2.5. Generation of H. mediterranei deletion mutants: HM26-Δlsm (R4 ΔpyrE2 Δlsm1) and HM26-ΔSm1 (R4 ΔpyrE2 ΔSm1)

#### 2.5.1. Generation of the lsm1 deletion strain

The HM26-Δ*lsm* deletion mutant (R4 Δ*pyrE2* Δ*lsm1*) was constructed using the pop-in/pop-out method described previously in *H. mediterranei* [43]. To delete the *lsm* open reading frame (HFX_RS09865), the upstream (570 bp) and downstream (520 bp) regions of the *lsm* gene were amplified by PCR [100 ng DNA

H. mediterranei R4, NH$_4^+$ buffer 1X, 3 mM MgCl$_2$, 0.2 mM dNTPs, 100 pmol/each primer, and 1 U BIOTAQ™ DNA Polymerase (Bioline, Buenos Aires, Argentina)] using primers LsmU1 and LsmU2 and LsmD1 and LsmD2, respectively (Supplementary Table 1). PCR products were purified using the IllustraTM GFX™ PCR DNA and Gel Band Purification Kit (GE Healthcare, Little Chalfont, UK) according to the manufacturer's instructions. The PCR products containing 18 identical nucleotides at one end were merged into a single fragment by subsequent fusion PCR [100 ng/each of purified PCR fragments, PCR buffer 1X, 1.5 mM MgSO$_4$, 0.2 mM dNTPs, 100 pmol/each primer (LsmU1 and LsmD2) and 1 U KOD Hot Start DNA Polymerase (Novagen, Merck, Darmstadt, Germany)], resulting in a fragment of 1071 nucleotides containing an in-frame deletion version of the *lsm* gene and its upstream and downstream regions. This fragment was cloned into the pMH101 N vector (suicide plasmid) [43] using restriction selection cloning [45]. The cloned sequence region was verified by Sanger sequencing (Stabvida, Caparica, Portugal), and the plasmid pMH101N-Δ*lsm* generated was used to transform *H. mediterranei* HM26 [43]. A defined uracil-free medium was utilised to select clones that had integrated pMH101N-Δ*lsm* into their genome via homologous recombination (pop-in clones). Subsequently, pop-out clones were selected in a complex medium supplemented with 750 µg/mL 5-fluoro-orotic acid (5-FOA), which is toxic to cells containing the *pyrE* gene. After the second recombination event (pop-out clones), the genome had either the wild-type copy or the *lsm* gene deletion. The genomic organisation of 100 pop-out clones and wild-type genes were analysed using PCR screening (LsmU1 and LsmD2 primers) and Southern blot analysis. The PCR was performed with 800 ng of genomic DNA, 1X PCR buffer, 1.5 mM MgCl$_2$, 0.16 mM dNTPs, 100 pmol/each primer, and 1 U BioThermStar DNA polymerase (Gene-Craft, Amsterdamer, Germany). For Southern blot analysis, genomic DNA (3 µg) was digested with *Afe*I (Thermo Fisher Scientific, Waltham, MA, USA) (Figure S1A). Prehybridisation, hybridisation (65 °C), and chemiluminescent detection were performed as described in the DIG Application Manual for filter hybridisation (Roche, Mannheim, Germany). The gene sequence of the *lsm* gene deletion mutant (HM26-Δ*lsm*) is shown in Fig. 1B.

2.5.2. Generation of the Sm1 motif deletion strain

The Sm1-encoding motif in the *lsm* gene (Fig. 1) was deleted in strain HM26 using the pop-in/pop-out method [43]. This deletion mutant contains an intact internal promoter of the *rpl37e* gene
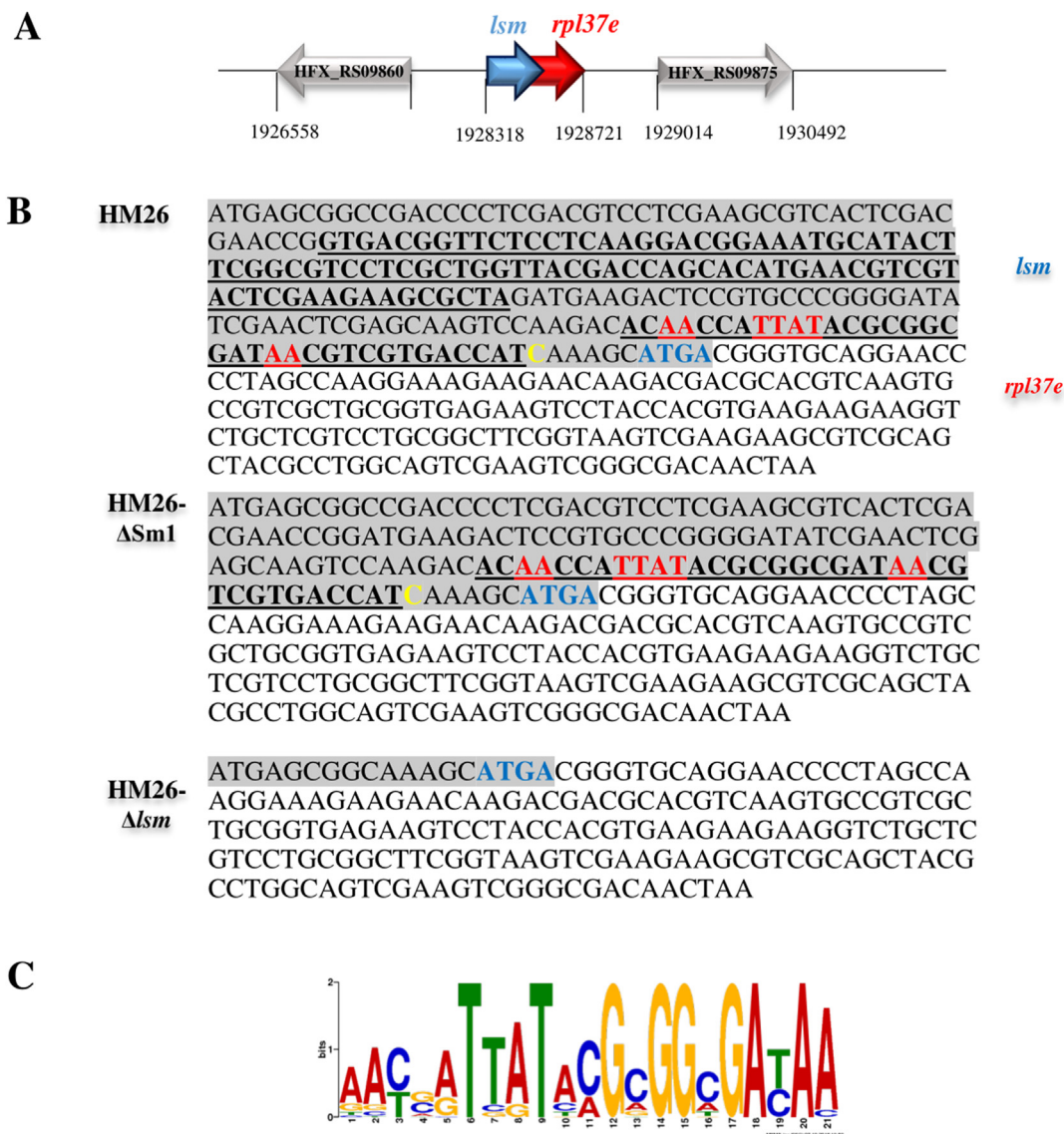
Fig. 1. The *lsm* gene in *H. mediterranei*. A. Genomic location. The operon containing the genes for *lsm* and *rpl37e* is bordered by the genes for a ribonuclease J (HFX RS09860) and an amidophosphoribosyltransferase (HFX RS09875). **B. *lsm* gene sequences in parental strain HM26, HM26-ΔSm1, and HM26-Δ*lsm*.** The open reading frames for the Lsm protein (shown in grey) and the ribosomal protein L37e (shown without shading) overlap by four nucleotides (bold blue). The Sm1-and Sm2-encoding motifs in the *lsm* gene are shown in bold and underlined black, respectively. The Sm2 motif of *lsm* contains the TATA box of the promoter for the *rpl37e* gene (bold red: AA-TTAT-AA). **C. The TATA-box sequence of the promoter of the *rpl37e* gene is located in Sm2 motif.** Sequence logos were generated by MEME SUITE from the 80 archaeal species.

located in the Sm2 motif. Chromosomal DNA from *H. mediterranei* R4 was used as a template. The upstream and downstream regions of the Sm1 coding region (each 1 kb long) were amplified by PCR [100 ng DNA *H. mediterranei* R4, NH$_4^+$ buffer 1X, 3 mM MgCl$_2$, 0.2 mM dNTPs, 100 pmol/each primer, and 1 U BIOTAQ™ DNA Polymerase (Bioline, Buenos Aires, Argentina)] using primers Sm1U1 and Sm1U2, and Sm1D1 and Sm1D2, respectively (for primer sequences see Supplementary Table 1). The PCR product Sm1Up and integrative pMH101 N were digested with *Kpn*I and *Hind*III and subsequently cloned to obtain plasmid pMH101-Sm1Up. To ligate the PCR product Sm1Down into pMH101-Sm1Up, it was digested with *Hind*III and *Bam*HI to obtain plasmid pMH101N-ΔSm1 (suicide plasmid of Sm1 motif). The cloned sequence region was verified by Sanger sequencing (Stabvida, Caparica, Portugal), and the *H. mediterranei* HM26 strain was transformed with the generated plasmid pMH101N-ΔSm1. Pop-in clones were selected by growth on uracil-free medium, and pop-

out was induced in a complex medium containing 750 μg/mL 5-FOA. The isolated DNA from 100 pop-out clones was amplified by PCR using primers Sm1U1 and Sm1D2 and examined by restriction analysis (*Hind*III) and Southern blot analysis. For Southern blot analysis, genomic DNA (3 μg) was digested with *Hind*III and *Nco*I (Thermo Fisher Scientific, Waltham, MA, USA) (Fig. S1B). Prehybridisation, hybridisation (65 °C), and chemiluminescent detection were performed as described above. The gene sequence of the Sm1 motif-deletion mutant (HM26-ΔSm1) is shown in Fig. 1B.

2.6. Northern blot analyses

Northern blot was performed to analyse the co-transcription of the *lsm* gene in HM26 and to confirm the expression of the *rpl37e* gene in the HM26-Δ*lsm* and HM26-ΔSm1 deletion mutants. Total RNA isolated from HM26-Δ*lsm* (10 μg per lane) was denatured and separated by electrophoresis (2 h, 100 V) using formaldehyde/1.2%

agarose gels in MOPS buffer (20 mM MOPS, pH 7.0, 5 mM sodium acetate, and 1 mM EDTA). The RNAs were transferred to a nylon membrane from the gel using a semi-dry electrophoretic transfer cell (30 min, 20 V) and fixed by drying the membrane overnight at room temperature. A digoxigenin-labelled DNA probe was generated by PCR using Dig-dUTP (20 μM) and a dNTP mix with reduced dTTP concentration (20 μM). The specific probe for the *rpl37e* gene was generated using the primers Rpl37eF/Rpl37eR, and a specific probe for the *lsm* gene was generated using the primers Lsm_north_F/Lsm_north_R (Table S1). For hybridisation, the membrane with cross-linked RNA samples was equilibrated in high SDS buffer [5xSSC, 2% (w/v) blocking reagent, 0.1% (w/v) N-lauroylsarcosine, 0.2% (w/v) SDS, 50% (w/v) formamide] (2 h, 50 °C), followed by incubation with 50 ng labelled probe per millilitre of high SDS buffer (overnight, 50 °C. The membrane was washed twice in 5xSCC/0.1% (w/v) SDS (5 min, room temperature) and twice in 2xSCC/0.1% (w/v) SDS (15 min, room temperature). DIG detection was performed with an alkaline phosphatase coupled anti-DIG antibody and the chemiluminescence substrate CSPD, according to the manufacturer's instructions (Roche, Mannheim, Germany). The signals were visualised on an X-ray film (GE Healthcare, Buckinghamshire, UK).

2.7. Phenotypic characterisation of deletion mutants: HM26-Δlsm (R4 ΔpyrE2 LSm) and HM26-ΔSm1 (R4 ΔpyrE2 ΔSm1)

2.7.1. Growth curves

H. mediterranei strains HM26 (R4 Δ*pyrE2*), HM26-Δ*lsm* (R4 Δ*pyrE2 lsm*), and HM26-ΔSm1 (R4 Δ*pyrE2* ΔSm1) were grown under different conditions, as mentioned in Table 1. Three biological replicates were generated. The average values of growth rate (μ) [$X = X_0 \, e^{\mu t}$; X_0 is the cell concentration at the beginning of the exponential growth phase, and X is the cell concentration after a time interval (t)], generation time ($td = ln \, 2/\mu$), lag-phase length, and standard deviations ($\sqrt{\frac{\sum (x-\bar{x})^2}{n}}$; x is the sample mean average, and *n* is the sample size) were calculated. Cell samples were collected in the mid-exponential and stationary phases of each culture medium for the different phenotypic characterisation assays.

2.7.2. Swarming assay

The swarming assays were performed using cell samples taken in the mid-exponential and stationary phases of the defined medium, which contained 40 mM KNO₃ or 40 mM NH₄Cl and supplemented with 10 g/L glucose, 0.0005 g/L FeCl₃, 0.5 g/L KH₂PO₄, 100 mM MOPS, and 50 μg/mL uracil. Cells were collected by centrifugation at 13000*g* for 10 min and resuspended in 25% SW to yield an OD₆₀₀ of 3.75 for equal cell densities. A 2 μL cell suspension of HM26-Δ*lsm,* HM26-ΔSm1, and the parental strain HM26 was added to the middle of the swarm plates (agar 0.3% (w/v) containing defined medium with 40 mM KNO₃ or 40 mM NH₄Cl. The plates were incubated at 42 °C, and the swarming radii were measured daily. Three or four biological replicates were analysed. The average values and standard deviations were calculated as described in 2.7.1.

2.7.3. Ethanol resistance assay

The ethanol resistance assays were performed in complex medium with or without 1% (v/v) ethanol from cells collected in the mid-exponential and stationary phases. Cells were collected by centrifugation at 13000*g* for 10 min and resuspended in 25% SW to yield an OD₆₀₀ of 3.75 to equalise cell densities. A 2 μL cell suspension consisting of HM26-Δ*lsm,* HM26-ΔSm1, and HM26 was added to the middle of swarm plates (agar 0.3% (w/v) containing complex medium or complex medium supplemented with 1% (v/v) ethanol. The plates were incubated at 42 °C, and the swarming radii were measured daily. At least three biological replicates were analysed. The average values, growth rates, survival percentage to ethanol stress [(radii ethanol/radii no-ethanol) x 100], and standard deviations were calculated as described in 2.7.1.

2.7.4. Heat stress assay

The heat stress assay was performed with 1 mL of cells (HM26-Δ*lsm,* HM26-ΔSm1, and HM26 strains) in a complex medium, collected in the mid-exponential and stationary phases. The cells were incubated at 65 °C for 15 min, 30 min, and 1 h, and then cooled on ice. The cells that did not receive heat treatment served as the control. The cells were plated on complex medium and incubated at 42 °C for 7 days to obtain CFU/mL of culture using a plate counting method. At least three biological replicates were analysed. The survival percentage to heat stress [(CFU after treatment/CFU no-treatment) × 100] and standard deviations were calculated as described in 2.7.1.

2.7.5. Oxidative stress assay

The oxidative stress assay was performed using 1 mL aliquots collected in the mid-exponential and stationary phases, using the complex medium of HM26-Δ*lsm,* HM26-ΔSm1, and HM26 strains. The cells were incubated in 2 mM H₂O₂ for 0 min (as a control), 15 min, 30 min, and 1 h and plated on complex medium at 42 °C for 7 days to obtain CFU/mL of culture using a plate counting method. At least three biological replicates were analysed. The survival percentage to oxidative stress [(CFU after treatment/CFU no-treatment) x 100] and standard deviations in the function of oxidative stress time were calculated as described in 2.7.1.

3. Results

3.1. Bioinformatics analysis of lsm gene in H. mediterranei

The gene encoding the Lsm protein was identified in the *H. mediterranei* ATCC 33500[T] genome [42] using a BLAST search [46] with the previously described archaeal Lsm protein in the genus *Haloferax* [14]. *H. mediterranei* contains a single *lsm* gene (HFX_RS09865), which encodes 76 amino acids with a theoretical molecular mass of 8.25 kDa and pI of 3.9. Sequence analysis of the Lsm protein showed that this protein belongs to the Lsm1 subfamily of Lsm proteins. The *lsm* gene overlaps by four nucleotides with the *rpl37e* gene, which encodes the L37e ribosomal protein (HFX_RS09870). In *H. volcanii,* the promoter of the *rpl37e* gene is located in the Sm2 motif of the *lsm* gene [36]; this promoter sequence is completely conserved in *H. mediterranei* (Fig. 1A). A BLAST search was used to analyse the sequence conservation of Lsm protein in the genomes of microorganisms belonging to the *Archaea* domain, specifically in the Euryarchaeota phylum. The multiple sequence alignments of *H. mediterranei* Lsm1 with 21 Lsm1 proteins of the Halobacteria class (Figure S2) and with 29 Lsm1 proteins of the Euryarchaeota phylum (Figure S3) showed that the protein is highly conserved in archaea, except for the regions outside the Sm1 and Sm2 domains, which correspond to β-sheets 3 and 4, respectively. Notably, the Sm1 and Sm2 motifs are highly conserved across the *Archaea* domain (Figures S2 and S3). Consequently, the promoter sequence of the *rpl37e* gene (AA-TTAT-AA) is also conserved (Fig. 1B). Moreover, Arg4, Pro5, Leu6, Asp7, Tyr34, and Asp35 residues form a specific binding pocket for uridine in *P. abyssi* [33], which are universally conserved (Figures S2, S3, and S4), indicating specific uridine binding in all archaeal Lsm proteins analysed.

Eighty archaeal genomes were examined to analyse the conservation of the gene order. In 77 of the 80 archaeal genomes

Fig. 2. Comparison of Lsm amino acid sequence of *H. mediterranei* with eukaryotic and bacterial sequence consensus. The grey shaded residues of the *H. mediterranei* Lsm protein corresponding to the residues of the consensus sequence. The red shaded residues of the *H. mediterranei* Lsm protein corresponding to the highly conserved residues of the consensus sequence. h: bulky, hydrophobic (V, I, L, M, F, Y, or W). The consensus sequences of eukaryotes and bacteria were obtained from Achsel et al., 1999 [49] and Sauer, 2013 [50].
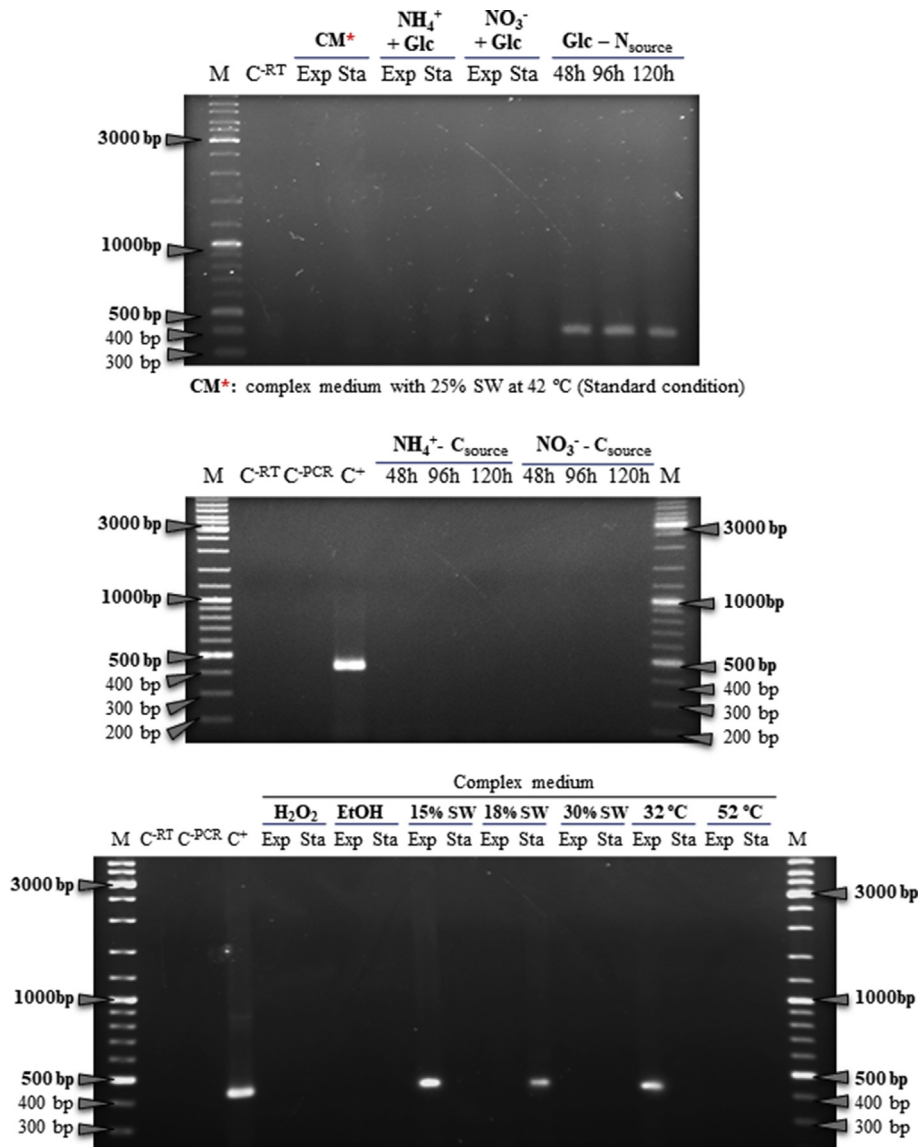
Fig. 3. Analysis of co-transcription of *lsm* and *rpl37e* genes under different culture media and growth conditions in *H. mediterranei* by reverse transcription-polymerase chain reaction (RT-PCR). The expected size of bicistronic transcript is 404 bp. M: GeneRuler Low Range DNA Ladder (Thermo Fisher Scientific, Waltham, MA, USA). C^{-RT}: negative control, without reverse transcriptase. C^{-PCR}: negative control, PCR prepared without cDNA. C+: positive control, PCR prepared with DNA isolated. **A.** CM*: complex medium with 25% SW at 42 °C (standard condition); NH$_4^+$ + Glc: defined medium (25 % SW) with 40 mM ammonium and 10 g/L glucose at 42 °C; NO$_3^-$ + Glc: defined medium (25% SW) with 40 mM nitrate and 10 g/L glucose at 42°C; Glc - N$_{source}$: defined medium (25% SW) with 10 g/L glucose without nitrogen source at 42 °C. **B.** NH$_4^+$ - C$_{source}$: Glc: defined medium (25 % SW) with 40 mM ammonium without carbon source at 42 °C; NO$_3^-$ - C$_{source}$: defined medium (25 % SW) with 40 mM nitrate without carbon source at 42 °C. **C.** H$_2$O$_2$: complex medium (25% SW) with 2 mM hydrogen peroxide at 42 °C; EtOH: Complex medium (25% SW) with ethanol 1% (v/v) at 42 °C; 15% SW: complex medium (15% SW) at 42 °C; 18% SW: complex medium (18% SW) at 42 °C; 30% SW: complex medium (30% SW) at 42 °C; 32 °C: complex medium (25% SW) at 32 °C; 52 °C: complex medium (25% SW) at 52 °C; Exp: exponential phase; Sta: stationary phase.
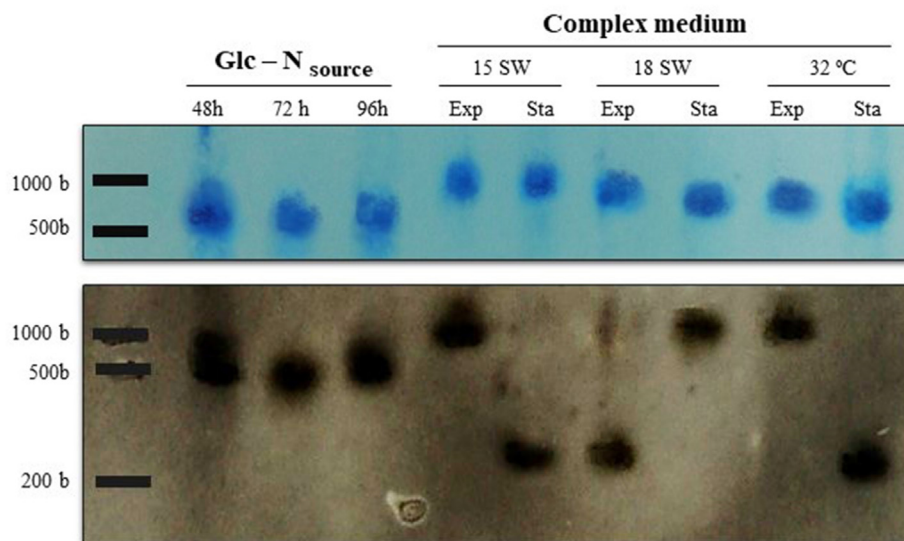
Fig. 4. Co-transcription of *lsm* and *rpl37e* genes in *H. mediterranei* by northern blot analysis with specific *lsm* probe. The upper part shows the stained RNA gel with the 16S ribosomal RNA band, while the lower part shows the signals of the northern blot. The expected size of the bicistronic transcript is 400 bases and that of the monocistronic transcript is 273 bases. M: RiboRuler High Range RNA Ladder (Thermo Fisher Scientific, Waltham, MA, USA). Glc - N$_{source}$: defined medium 25% SW with 10 g/L glucose without nitrogen source at 42 °C; 15% SW: complex medium (15% SW) at 42 °C; 18% SW: complex medium (18% SW) at 42 °C; 30% SW: complex medium (30% SW) at 42 °C; 32 °C: complex medium (25% SW) at 32 °C. Exp: exponential phase; Sta: stationary phase.

analysed, *lsm* and *rpl37e* genes are consecutively encoded and transcribed in the same direction. In 56 genomes, the two genes overlap (by one or four nucleotides), and in 21 genomes, they are very closely spaced (6—495 nucleotides) (Table S2). These results indicate that the gene order is highly conserved in archaea, and co-transcription, as part of the conserved operon by a joint promoter, can be assumed. Moreover, *lsm* and *rpl37e* co-transcription has already been demonstrated experimentally in *H. volcanii* [36].

Halophilic archaeal proteins are characterised by an increase in the number of acidic residues and a decrease in that of basic residues compared to their mesophilic counterparts [47,48]. Curiously, the percentage of similarity between *H. mediterranei* and eukaryotic species is more than 45% (Figure S5). The Lsm amino acid sequence of *H. mediterranei* corresponds precisely to the amino acid sequence consensus of eukaryotic Lsm proteins [49]. At the same time, it only presents some similarities with the sequence consensus of bacterial Hfq proteins [50] (Fig. 2).

3.2. Transcriptional expression and co-transcription of lsm and rpl37e genes

RT-PCR analyses were performed using RNA from cells cultivated under different conditions to determine the transcripts of *lsm* and *rpl37e* genes and the co-transcription of both. As expected, the *rpl37e* gene, which encodes a ribosomal protein, is expressed in all conditions tested during the exponential and stationary growth phases (Figure S6). In contrast, the *lsm* gene was expressed in all conditions except in a defined medium with 40 mM nitrate as a nitrogen source and carbon starvation at different times (48, 96, and 120 h) (Figure S7). Both genes were co-transcribed under various conditions (Fig. 3). The co-transcription of *lsm* and *rpl37e* genes occurred during nitrogen starvation throughout growth (Fig. 3A). Simultaneously, co-transcription occurred during carbon starvation, regardless of the nitrogen source (ammonium or nitrate) (Fig. 3B). Under the stress conditions tested (Fig. 3C), co-transcription depended on the SW concentration and temperature. However, co-transcription did not occur under oxidative stress conditions (2 mM H$_2$O$_2$) or in the presence of ethanol (1%, v/v). Specifically, both genes were co-transcribed in a complex medium

with 15% SW in the exponential phase, in a complex medium with 18% SW in the stationary phase, and in the complex medium at 32 °C in the exponential phase. These results indicate that *lsm* and *rpl37e* co-transcription occurs at SW concentrations and temperatures lower than those required for optimal growth (25% SW and 42 °C), depending on the growth phase.

The RT-PCR technique allows the analysis of co-transcription of *lsm* and *rpl37e* genes; however, it is not possible to determine whether a monocistronic transcript is also expressed. Therefore, the conditions under which co-transcription occurs were analysed by northern blotting using a probe specific to the *lsm* gene. These results indicate that under the conditions where co-transcription takes place, only a bicistronic transcript is expressed (Fig. 4).

3.3. Deletion of the lsm gene and Sm1 motif

The *lsm* deletion mutant (HM26-Δ*lsm*) and the Sm1 motif deletion mutant (HM26-ΔSm1) were generated using the pop-in/pop-out method to determine the biological function of the archaeal Lsm protein. The genomic organisation of the pop-out clones (HM26-Δ*lsm* and HM26-ΔSm1) and parental strain (HM26) are shown in the supplementary material (Figure S1). Thirty percent of HM26-Δ*lsm* pop-out clones screened and 10% of HM26-ΔSm1 pop-out clones screened presented the deleted version. PCR screening, restriction analysis, and Southern blotting revealed that the mutants were successfully constructed (Figure S8); therefore, the *lsm* gene and the Sm1 domain are not essential in *H. mediterranei*. Northern blot analyses were performed to confirm the expression of the *rpl37e* gene in the HM26-Δ*lsm* and HM26-ΔSm1 deletion mutants. The results indicate that the *rpl37e* gene is expressed in all conditions tested in both deletion mutants; therefore, the deletion of the *lsm* gene and Sm1 motif does not affect its expression (Fig. 5).

3.4. Phenotypic characterisation of deletion mutants: HM26-Lsm (R4 ΔpyrE2 Δlsm1) and HM26-Sm1 (R4 ΔpyrE2 ΔSm1)

3.4.1. Growth curves

The growth of HM26-Δ*lsm*, HM26-ΔSm1, and HM26 was
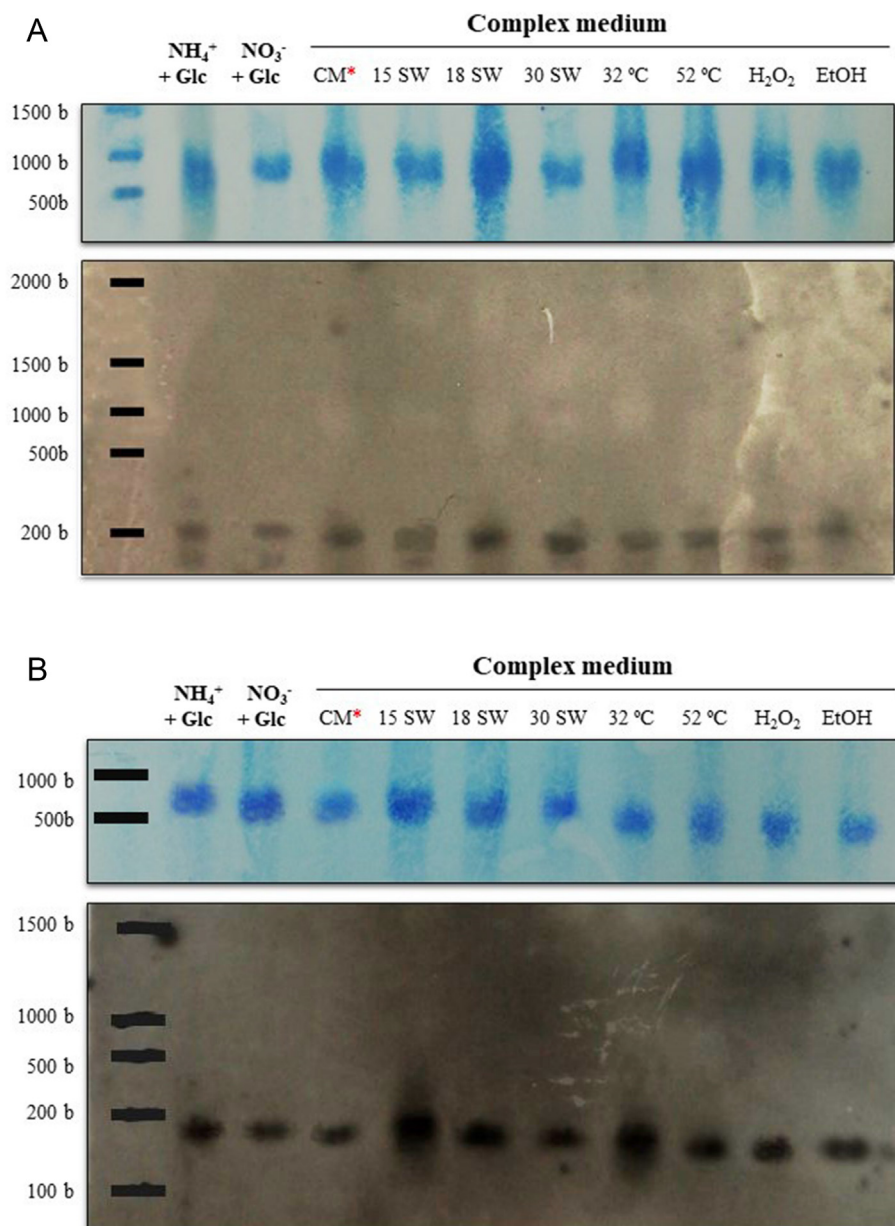
Fig. 5. Expression of the *rpl37e* gene in HM26-Δ*lsm* (A) and HM26-ΔSm1 (B) deletion mutants by northern blot analysis. The upper part shows the stained RNA gel with the 16S ribosomal RNA band, while the lower part shows the signals of the northern blot. The expected size is 177 bp. M: RiboRuler High Range RNA Ladder (Thermo Fisher Scientific, Waltham, MA, USA). NH_4^+ + Glc: defined medium 25% SW with 40 mM ammonium and 10 g/L glucose at 42 °C; NO_3^- + Glc: defined medium (25% SW) with 40 mM nitrate and 10 g/L glucose at 42 °C; CM*: complex medium with 25% SW at 42 °C (standard condition); 15% SW: complex medium (15% SW) at 42 °C; 18% SW: complex medium (18% SW) at 42 °C; 30% SW: complex medium (30% SW) at 42 °C; 32 °C: complex medium (25% SW) at 32 °C; 52 °C: complex medium (25% SW) at 52 °C; H_2O_2: complex medium (25% SW) with 2 mM hydrogen peroxide at 42 °C; EtOH: complex medium (25% SW) with 1% (v/v) ethanol at 42 °C.

analysed in the presence of different nitrogen sources. The HM26-Δ*lsm* and HM26-ΔSm1 deletion mutants and the parental strain HM26 showed no growth differences in defined media in the presence of 40 mM ammonium; however, HM26-ΔSm1 presented a more extended lag phase in 40 mM nitrate as a nitrogen source (Figure S9). Comparison of HM26-ΔSm1, HM26-Δ*lsm,* and HM26 under standard growth conditions (complex medium with 25% SW at 42 °C) revealed that the HM26-Δ*lsm* mutant exhibited a lower growth rate and reached lower optical densities (Fig. 6A). According to the salt concentration, the growth curve of the three strains revealed that the growth of HM26-Δ*lsm* was not as optimal as that of the parental strain HM26 at all salt concentrations tested, except for 18% SW, while the HM26-ΔSm1 and HM26 strains had similar

growth profiles (Fig. 6A–D). The comparison of HM26-ΔSm1, HM26-Δ*lsm,* and HM26 at different temperatures showed that HM26-Δ*lsm* reached lower optical densities at 32 °C (Figs. 6E) and 42 °C (Fig. 6A), while HM26-ΔSm1 and HM26 had similar growth profiles. When the temperature increased, the growth was independent on the strain (Fig. 6F). Curiously, the effect was reversed in the presence of ethanol stress, as HM26-Δ*lsm* showed a higher growth rate than HM26-ΔSm1 and HM26 (Fig. 6G). Finally, the growth of the parental strain HM26 was more affected by oxidative stress compared to the mutant strains (Fig. 6H). These results establish that the growth capabilities of the mutant and wild-type strains under various conditions were variable, presenting phenotypic differences. The growth rates and optical densities at the
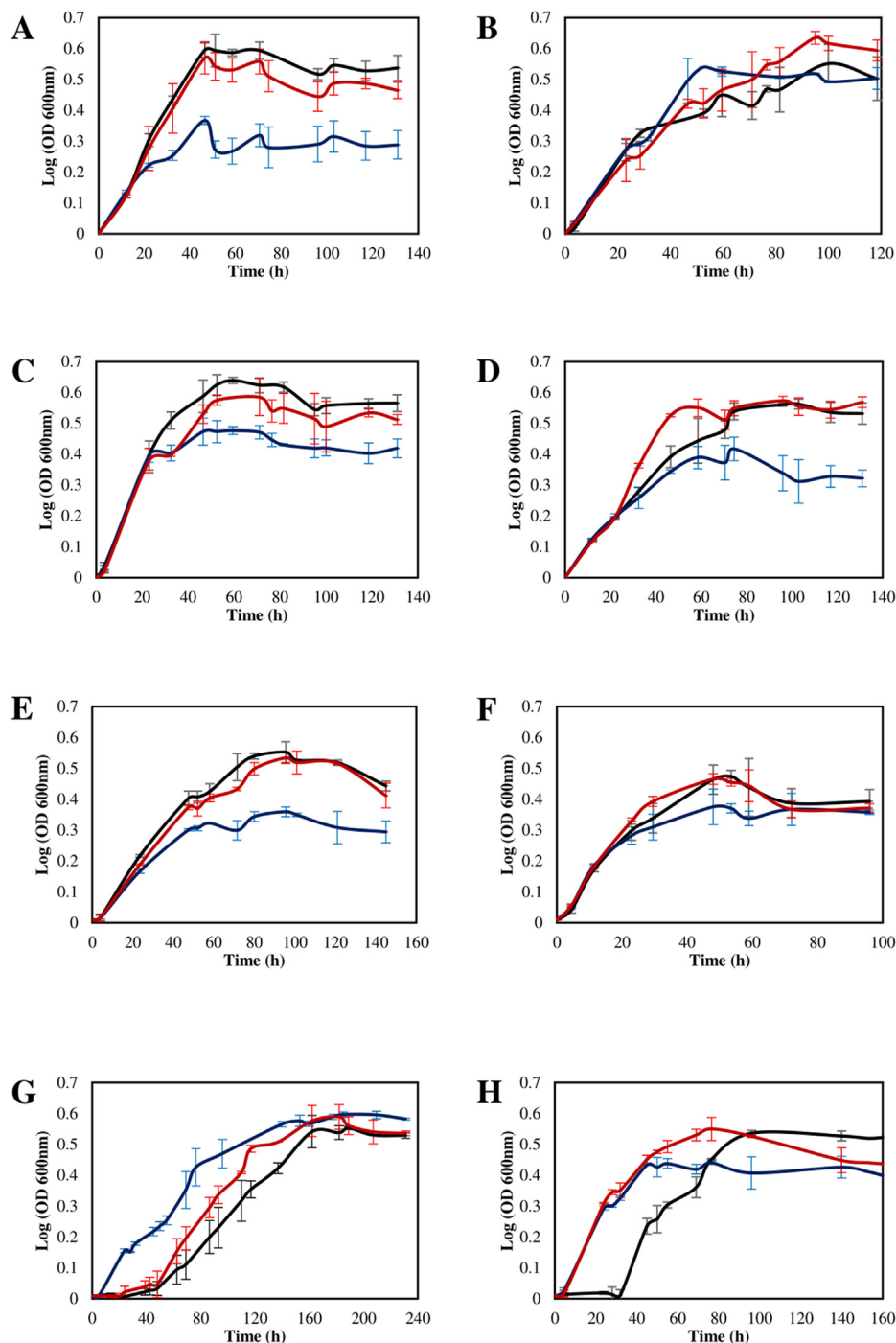
Fig. 6. Growth curves of deletion mutants (HM26-ΔSm1 and HM26-Δ*lsm*) and parental strain (HM26). A. Complex medium (25% SW) at 42 °C, (standard condition). **B.** Complex medium (15% SW) at 42 °C. **C.** Complex medium (18% SW) at 42 °C. **D.** Complex medium (30% SW) at 42 °C. **E.** Complex medium (25% SW) at 32 °C. **F.** Complex medium (25% SW) at 52 °C. **G.** Complex medium (25% SW) with 1% (v/v) ethanol at 42 °C. **H.** Complex medium (25% SW) with 2 mM H_2O_2 at 42 °C. HM26 (● , black), HM26-ΔSm1 (● , blue) and HM26-Δ*lsm* (● , red).

stationary phase as well as generation times were calculated (Table S3).

3.4.2. Swarming assay according to nitrogen source

The swarming assay revealed that the mutant strains presented a significantly greater swarming ability than HM26 from 144 h at 42 °C (Fig. 7, Table S3). Moreover, this result was observed independent of the nitrogen source (Fig. 7A–D). This experiment was performed using cell samples at exponential and stationary growth phases, and no significant differences were observed in swarming abilities according to the growth phase (Figure S10, Table S4).

3.4.3. Ethanol resistance assay

The ethanol resistance assays were performed in complex medium with or without 1% (v/v) ethanol from cells taken in the middle of the exponential and stationary phases. The radii (cm) of HM26, HM26-ΔSm1, and HM26-Δ*lsm* were smaller in the complex medium with ethanol than in the complex medium. However,
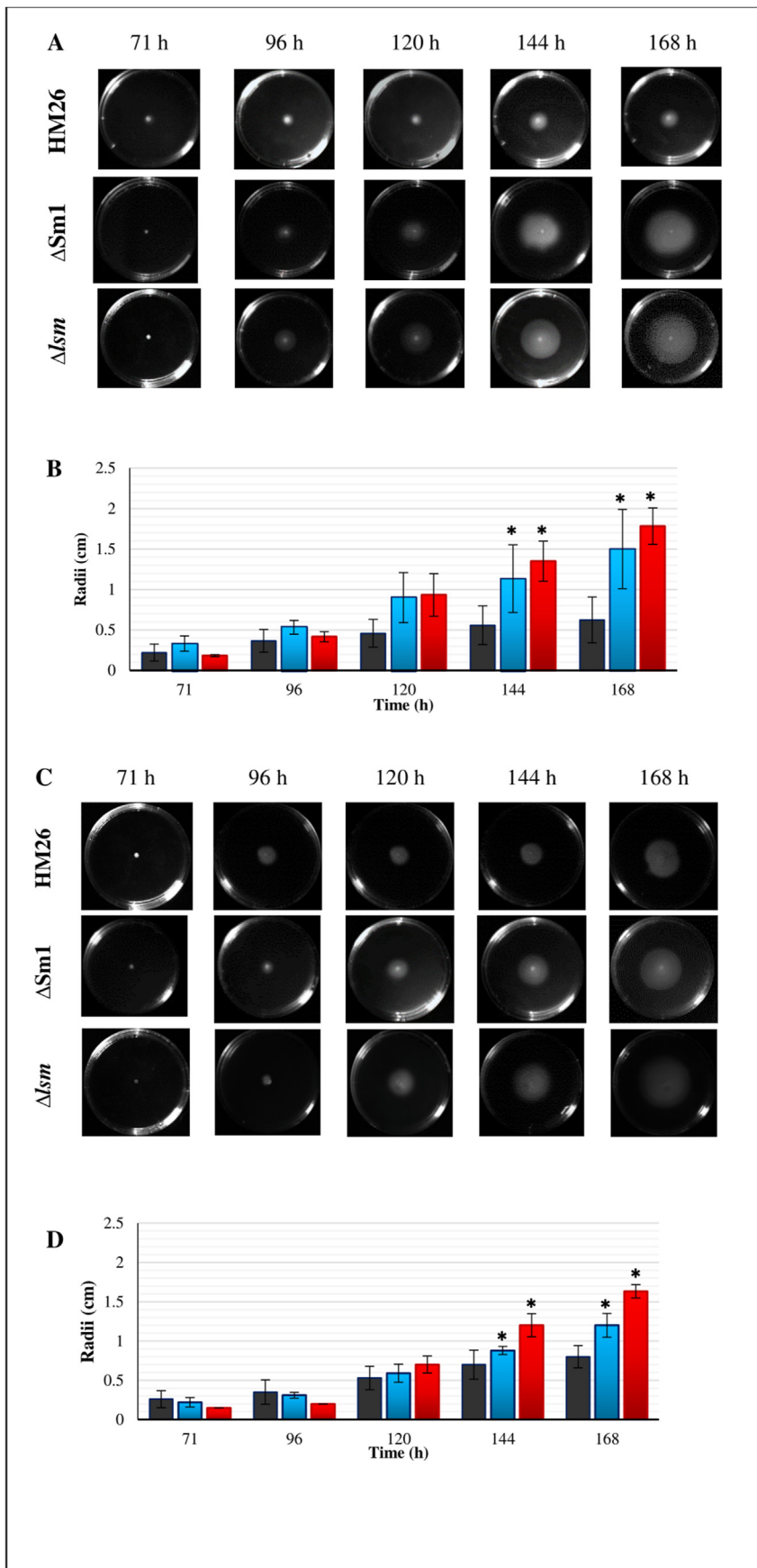
significant differences were observed only for HM26 and HM26-ΔSm1 (Fig. 8A, Table S5). These results suggest that HM26-Δ*lsm* is more resistant to ethanol than HM26 and HM26-ΔSm1. The survival percentage ([(radii ethanol/radii no-ethanol) x 100]) of HM26-Δ*lsm* was significantly higher than that of the parental strains HM26 and HM26-ΔSm1, which supports the results obtained (Fig. 8B, Table S6). No significant differences in ethanol resistance were observed according to the growth phase (Figure S11, Table S7).

3.4.4. Heat stress assay

Heat survival (65 °C) of HM26, HM26-ΔSm1, and HM26-Δ*lsm* was analysed at different time points (15, 30, and 60 min) from cells in the exponential and stationary phases (Fig. 9, Tables S8 and S9). The HM26-Δ*lsm* mutant showed significantly reduced survival percentage (<1%) at 15 min of treatment, both in the exponential and stationary phases (Fig. 9). These results indicate that HM26-Δ*lsm* is more sensitive to heating than HM26-ΔSm1 and HM26, regardless of the cell growth phase. In both the exponential and stationary phases, no significant differences were observed between HM26-ΔSm1 and HM26 at 15 min and 30 min after treatment. In contrast, HM26-ΔSm1 presented a significantly higher survival percentage at 60 min, both in the exponential and stationary phases, compared to HM26. These results suggest that HM26-ΔSm1 is more resistant to heating than the parental strain HM26 when the heat shock lasted for more than 30 min.

3.4.5. Oxidative stress assay

The oxidative stress resistance (H_2O_2 2 mM) of HM26, HM26-ΔSm1, and HM26-Δ*lsm* was analysed at different times (15, 30, and 60 min) from cells in the exponential and stationary phases. As expected, the survival of the parental strain HM26 was higher in the exponential phase than in the stationary phase because of the cell state. However, no differences were observed in HM26-Δ*lsm*, and the survival of HM26-ΔSm1 was higher in the exponential phase than in the stationary phase after 15 min of treatment. In contrast, no differences were observed in survival after treatment for 30 and 60 min (Fig. 10A, Table S11). The oxidative stress survival of HM26-Δ*lsm* and HM26-ΔSm1 was significantly lower than that of HM26 at 15 min after treatment versus HM26 from cells in the exponential and stationary phases (Fig. 10B, Table S12). These results suggest that both deletion mutants are more sensitive to oxidative stress than the parental strain.

4. Discussion

H. mediterranei contains a single *lsm* gene that overlaps by four nucleotides with the *rpl37e* gene, which encodes the L37e ribosomal protein. The *lsm* gene is adjacent to the *rpl37e* gene in most archaea genomes analysed (95.25%). Gene order in prokaryotes is considerably less conserved than protein sequences. Only a few operons, typically those that encode physically interacting proteins, are conserved in most bacterial and archaeal genomes. It might be assumed that the conserved gene-environment is co-regulated, constituting operons, even when they contain additional promoters [51,52]. Moreover, the Lsm and L37e ribosomal proteins might interact to regulate translation. The homologous protein Hfq cooperates with ribosomal proteins [53], playing a role in controlling the initiation of translation by binding at or near the ribosome binding site [54] and may act as a novel auxiliary factor in ribosome

biogenesis [55]. However, to date, there is no evidence of such interactions in any archaeal species.

The co-transcription of *lsm* and *rpl37e* genes has been confirmed in *H. mediterranei* with a single bicistronic transcript detected under different conditions: (i) under nitrogen starvation at different times (48, 96, and 120 h), (ii) in complex medium with 15% salt concentration in the exponential phase, (iii) in complex medium with 18% salt concentration in the stationary phase, and (iv) in the complex medium at 32 °C in the exponential phase. These results indicate that *lsm* and *rpl37e* co-transcription occurs at SW concentrations and temperatures lower than those required for optimal growth (25% SW and 42 °C) and depends on the growth phase. The *lsm* and *rpl37e* gene sequences are very similar to *H. volcanii,* but the expression conditions are different; for example, *lsm* and *rpl37e* are co-transcribed at high NaCl concentrations, and *lsm* and *rpl37e* are not expressed at 30 °C in *H. volcanii* [14]. Therefore, *lsm* and *rpl37e* expression and co-transcription occur differently in species of the same genus. Moreover, the *lsm* and *rpl37* genes are co-expressed as a bicistronic mRNA, and a monocistronic *rpl37R* transcript is detected.

In contrast, a monocistronic *lsm* transcript was not detected under the tested conditions in *H. volcanii* [36]. Instead, in *H. mediterranei*, the *lsm* and *rpl37e* genes are expressed under all conditions, and the *lsm* gene is expressed as a monocistronic transcript under most conditions because there is no co-transcription. These results suggest that *lsm* and *rpl37e* genes are expressed as monocistronic transcripts by different promoters located upstream of each gene, whereas co-transcription only occurs under certain stress conditions (nitrogen starvation, low salt concentration, and low temperature). Some archaeal genes are transcribed as polycistronic or monocistronic mRNA depending on the conditions, specifically in *H. mediterranei* [56] and *Methanosarcina thermophila* [57]. The regulatory mechanism of gene transcription in monocistronic and polycistronic transcription remains to be analysed in *H. mediterranei*.

Archaeal Lsm interacts with several proteins associated with translation, nucleic acid metabolism, stress-related and cell cycle, and several sRNAs, suggesting their involvement in different cellular pathways and their versatility [14]. According to the results of Fischer et al., 2010 [14], the *lsm* gene is expressed in many conditions and can interact with different proteins and sRNAs depending on the environmental conditions. Moreover, *rpl37e* is likely a constitutive gene, as it is expressed under all tested conditions. The *lsm* deletion mutant (*lsm* gene with a specific *rpl37e* promoter deleted) and the Sm1 motif deletion mutant were successfully generated in *H. mediterranei*; therefore, the *lsm* gene is not essential for this microorganism, even though it is involved in many cellular processes. The Sm1 deletion mutant showed growth differences compared to the parental strain under the highest and lowest salt tested concentrations and under oxidative stress conditions, which suggests that Lsm plays a crucial role in regulating these stress conditions.

Moreover, the Sm1 deletion mutant showed no differences in the defined media in the presence of 40 mM ammonium with the parental strain but presented a more prolonged lag phase in 40 mM nitrate as a nitrogen source. This outcome might indicate that Lsm is involved in the regulation of nitrogen assimilation. This could be required for optimal nitrate assimilation described in the cyanobacterium *Anabaena* sp. strain PCC 7120 [58]. As expected, the *lsm*

Fig. 7. Swarming assay of deletion mutants and HM26 according to nitrogen source from cells at exponential phase. HM26 (black), HM26-ΔSm1 (blue), and HM26-Δ*lsm* (red). **A.** Images of swarming plates with 40 mM ammonium at different times. **B.** The swarming radii at different times on plates with 40 mM ammonium. **C.** Images of swarming plates with 40 mM nitrate at different times. **D.** The swarming radii at different times on plates with 40 mM nitrate. * Statistically significant differences based on the Student's t-test between the deletion mutant (HM26-ΔSm1 or HM26-Δ*lsm*) and parental strain (HM26) (*p*-value < 0.05).
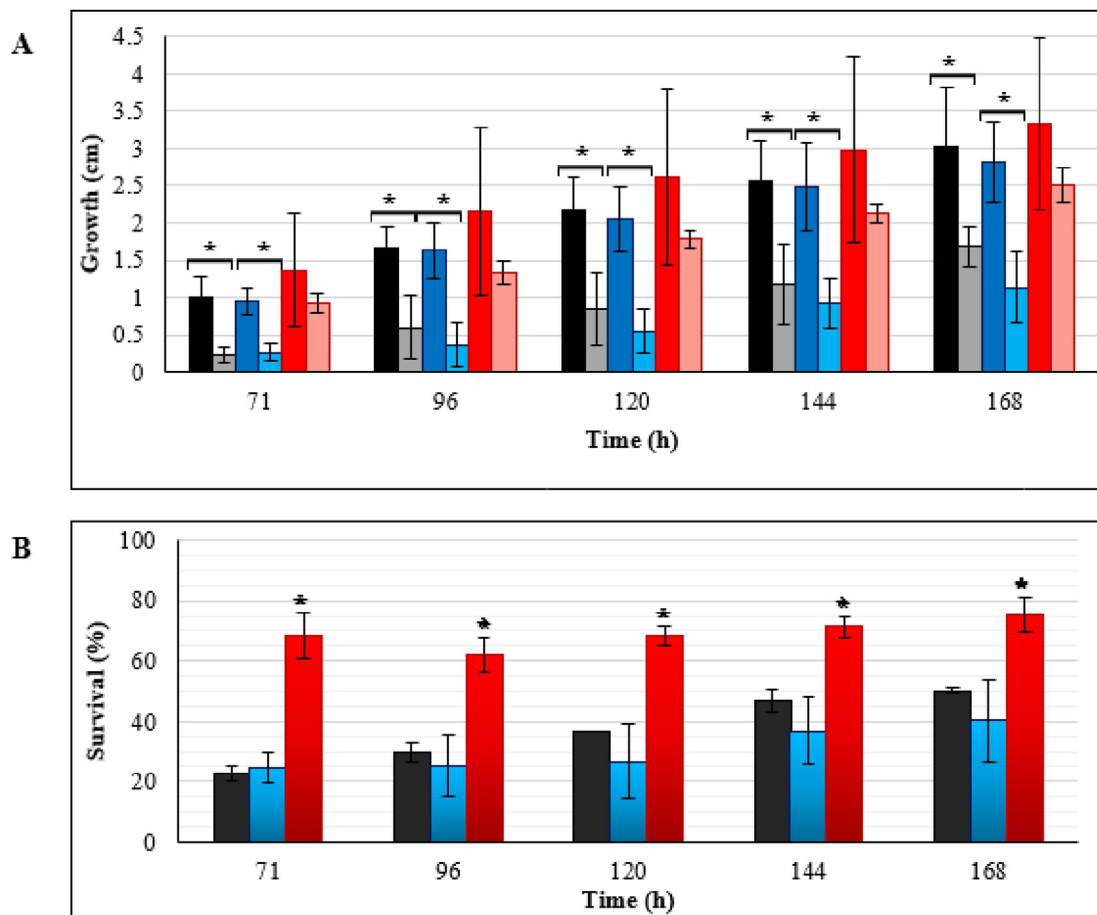
Fig. 8. Ethanol resistance assay of deletion mutants and HM26 from cells at the exponential phase. A. Growth of HM26 (black), HM26-ΔSm1 (blue), and HM26-Δ*lsm* (red) at different times in complex medium (dark colours) and complex medium with ethanol 1% (v/v) (light colours) plates. * Statistically significant differences based on the Student's t-test between complex medium and complex medium with ethanol (*p*-value < 0.05). **B.** Survival percentage of HM26 (black), HM26-ΔSm1 (blue), and HM26-Δ*lsm* (red) at different times. Statistically significant differences based on the Student's t-test between the deletion mutant (HM26-ΔSm1 or HM26-Δ*lsm*) and parental strain (HM26) (*p*-value < 0.05).

deletion mutant exhibited severe growth differences compared with the parental strain under all the tested conditions, unlike the Sm1 deletion mutant, because of the deletion of the complete *lsm* gene and specific *rpl37e* promoter.

Cellular motility is shown to be negatively affected in several studies of Hfq deletion mutants [59—62]. However, there are no studies related to motility in deletion mutants of the complete *lsm* gene in archaea species. Interestingly, both deletion mutants exhibited greater motility in the presence of different nitrogen sources compared to the parental strain HM26. Deletion mutants of the Sm1 motif in the *lsm* gene resulted in enhanced swarming activity in the presence of two carbon sources, and genes related to motility were upregulated in *H. volcanii* [36]. According to Maier et al., 2015 [36], the deletion of Sm1 might stress the cell, inducing the movement to search for better environmental conditions. This hypothesis agrees with our results, given the fact that the *lsm* deletion mutant presents more swarming ability and is more stressed than the Sm1 deletion mutant.

The interaction of sRNAs or several proteins, including cell cycle and stress-related proteins, with Lsm has been described in the *Archaea* domain [14]. In addition, sRNAs might regulate the expression of motility genes. For example, one archaeal sRNA gene deletion mutant presents increased swarming motility [63], and one bacterial sRNA regulates motility and biofilm formation in response to changes in nutrient availability [64]. Therefore, these results suggest that the Lsm protein of *H. mediterranei* could be involved in swarming activity by regulating sRNAs related to motility or regulating cell cycle or stress proteins.

The bacterial homolog Hfq regulates the response to different stress conditions, such as heat shock, oxidative stress, osmotic stress, UV exposure, acid pH, and ethanol stress [22,26—30]. However, no study has been performed concerning the involvement of Lsm proteins in archaeal species under stress conditions. The growth of Hfq deletion mutants was inhibited in the presence of ethanol, indicating that Hfq contributes to ethanol tolerance [30]. Unexpectedly, survival of the *H. mediterranei lsm* deletion mutant after ethanol exposure was significantly higher than that of the parental strain, while there were no significant differences between the Sm1 deletion mutant and the parental strain. All these data agree with the growth of *H. mediterranei lsm* deletion mutant in liquid medium in the presence of ethanol, resulting in a shorter lag phase. In addition, the sRNA gene deletion mutant in *H. volcanii* presents increased swarming motility in the presence of ethanol, which might be involved in the negative regulation of motility [63]. In this case, the Sm1 motif lacking in the Sm1 deletion mutant might be necessary to control the ethanol stress response in *H. mediterranei* via sRNA or protein regulation.

Furthermore, decreased survival after the thermal shock was observed in *hfq* deletion mutants in different bacterial species [26—28]. In our study, the Lsm mutant and the specific *rpl37e* promoter (HM26-Δ*lsm*) showed significantly decreased survival percentage less than 1% after 15 min of treatment. However, the
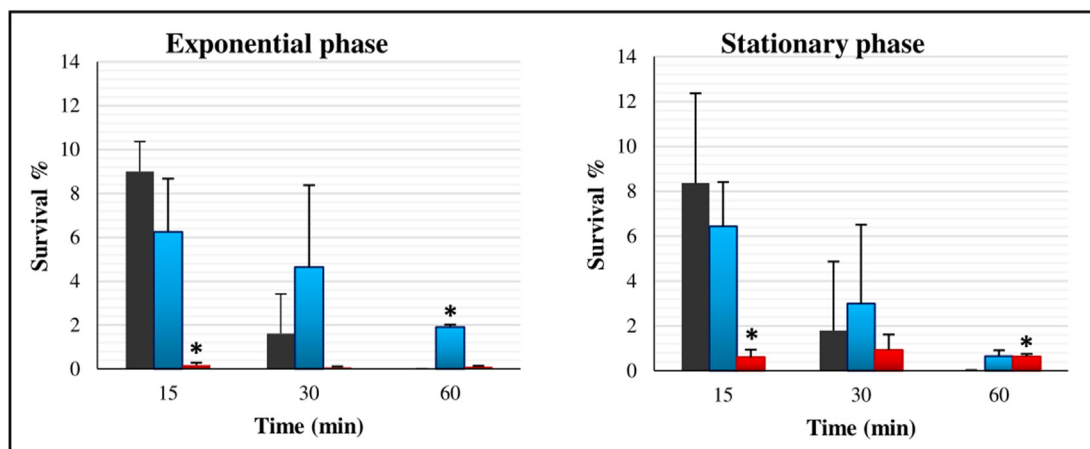
Fig. 9. Effect of heat shock (65 °C) at different incubation times in deletion mutants and parental strain HM26 in exponential phase (A) and stationary phase (B). Survival percentage ([(CFU after treatment/CFU no-treatment) x 100]) of HM26 (black), HM26-ΔSm1 (blue), and HM26-Δ*lsm* (red). Statistically, significant differences were based on the Student's t-test among deletion mutant (HM26-ΔSm1 or HM26-Δ*lsm*) and parental strain (HM26) (*p*-value < 0.05).
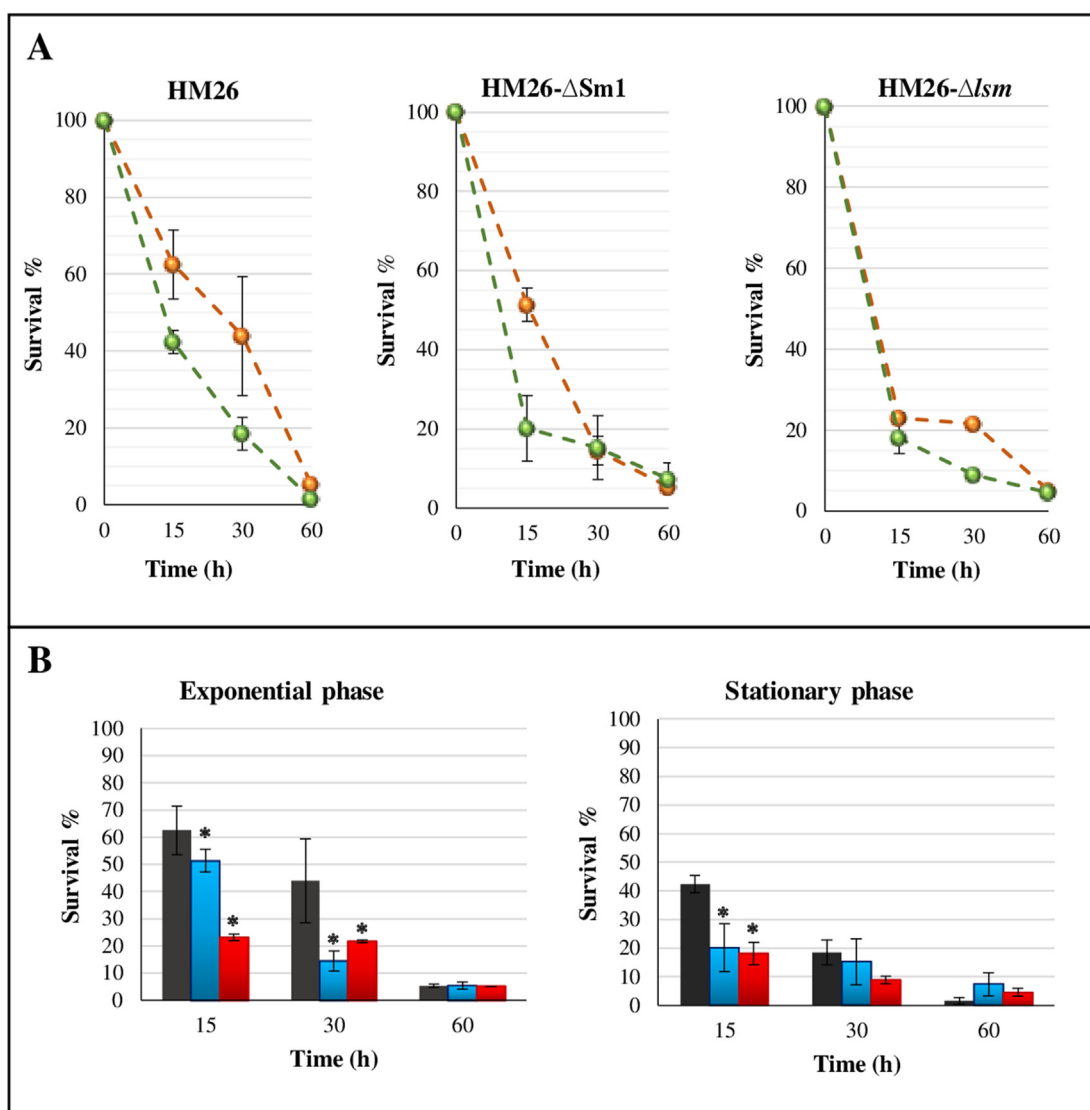
Fig. 10. Effect of oxidative stress (2 mM H_2O_2) at different incubation times in deletion mutants and parental strain HM26. A. Survival percentage of HM26, HM26-ΔSm1 and HM26-Δ*lsm* from cells at exponential phase (orange) and stationary phase (green). **B.** Survival percentage of HM26 (black), HM26-ΔSm1 (blue) and HM26-Δ*lsm* (red) from cells at exponential phase and stationary phase. The percentage of survival was calculated from the following formula ([(CFU after treatment/CFU no-treatment) x 100]). Statistically significant differences based on the Student's t-test among deletion mutant (HM26-ΔSm1 or HM26-Δ*lsm*) and parental strain (HM26) (*p*-value < 0.05).

mutant that only affected the Lsm protein (HM26-ΔSm1) showed better thermal shock resistance after 1 h of treatment. This result suggests that Lsm protein is involved in regulating the heat stress response in the short term. In particular, the Sm1 motif is necessary for this response. Besides, the oxidative stress resistance of HM26 and HM26-ΔSm1 depends on the growth phase, while HM26-Δ*lsm* presents a similar survival rate, independent of the growth phase. The oxidative stress survival of HM26-Δ*lsm* and HM26-ΔSm1 was significantly lower than that of HM26 from 15 min after cell treatment in the exponential and stationary phases. This result establishes that both deletion mutants are more sensitive to oxidative stress than the parental strain, which means that Lsm regulates the oxidative stress response in *H. mediterranei hfq* deletion mutants in different bacterial species [26,27,29].

5. Conclusion

The present study analysed the *lsm* gene from the extreme haloarchaeon *H. mediterranei* under different conditions, including various nitrogen sources and stress conditions. The results showed that the *lsm* gene and the overlapping *rpl37e* gene are co-transcribed, but their expression is regulated independently. Deletion mutants of the *lsm* gene and Sm1 motif were generated and extensively characterised under the same conditions to investigate the metabolic processes in which the Lsm protein plays an essential role. Our results suggest that Lsm protein plays a crucial role in regulating these stress conditions (low/high salinity, low/high temperature, heat shock, oxidative stress, and ethanol stress).

Funding

Author contributions

G.P and V.B conceived and designed the experiments; G.P performed most of the experiments; G.P analysed the data; V.B, M.C, M.-J.B, and J.E supervised the experimental work; G.P wrote original draft preparation; V.B, M.C, M.-J.B, and J.E reviewed and edited the manuscript; M.-J.B, project administration.

Declaration of competing interest

The authors declare that the research was conducted in the absence of any commercial or financial relationships that could be constructed as a potential conflict of interest.

Appendix A. Supplementary data

Supplementary data to this article can be found online at https://doi.org/10.1016/j.biochi.2021.05.002.

References

[1] B. Seraphin, Sm and Sm-like proteins belong to a large family: identification of proteins of the U6 as well as the U1, U2, U4 and U5 snRNPs, EMBO J. 14 (1995), 2089e2098.

[2] D.G. Scofield, M. Lynch, Evolutionary diversification of the Sm family of RNA-associated proteins, Mol. Biol. Evol. 25 (2008), 2255e2267, https://doi.org/10.1093/molbev/msn175.

[3] J. Vogel, B.F. Luisi, Hfq and its constellation of RNA, Nat. Rev. Microbiol. 9 (2011), 578e589, https://doi.org/10.1038/nrmicro2615.

[4] C. Sauter, J. Basquin, D. Suck, Sm-like proteins in Eubacteria: the crystal structure of the Hfq protein from *Escherichia coli*, Nucleic Acids Res. 31 (2003) 4091—4098, https://doi.org/10.1093/nar/gkg480.

[5] J.S. Nielsen, A. Bøggild, C.B. Andersen, G. Nielsen, A. Boysen, D.E. Brodersen, P. Valentin-Hansen, An Hfq-like protein in archaea: crystal structure and functional characterization of the Sm protein from *Methanococcus jannaschii*, RNA 13 (2007) 2213—2223, https://doi.org/10.1261/rna.689007.

[6] C. Wilusz, J. Wilusz, Eukaryotic Lsm proteins: lessons from bacteria, Nat. Struct. Mol. Biol. 12 (2005) 1031−1036, https://doi.org/10.1038/nsmb1037.

[7] P. Valentin-Hansen, M. Eriksen, C. Udesen, The bacterial Sm-like protein Hfq: a key player in RNA transactions, Mol. Microbiol. 51 (6) (2004) 1525−1533, https://doi.org/10.1111/j.1365-2958.2003.03935.x.

[8] M.A. Schumacher, R.F. Pearson, T. Møller, P. Valentin-Hansen, R.G. Brennan, Structures of the pleiotropic translational regulator Hfq and an Hfq-RNA complex: a bacterial Sm-like protein, EMBO J. 21 (2002), 3546e3556, https://doi.org/10.1093/emboj/cdf322.

[9] I. Törö, J. Basquin, H. Teo-Dreher, D. Suck, Archaeal Sm proteins form hepta-meric and hexameric complexes: crystal structures of the Sm1 and Sm2 proteins from the hyperthermophile *Archaeoglobus fulgidus*, J. Mol. Biol. 320 (2002) 129—142, https://doi.org/10.1016/S0022-2836(02)00406-0.

[10] T. Achsel, H. Stark, R. Lührmann, The Sm domain is an ancient RNA-binding motif with oligo(U) specificity, Proc. Natl. Acad. Sci. U.S.A. 98 (2001) 3685−3689, https://doi.org/10.1073/pnas.071033998.

[11] B.M. Collins, S.J. Harrop, G.D. Kornfeld, I.W. Dawes, P.M. Curmi, B.C. Mabbutt, Crystal structure of a heptameric Sm-like protein complex from archaea: implications for the structure and evolution of snRNPs, J. Mol. Biol. 309 (2001) 915−923, https://doi.org/10.1006/jmbi.2001.4693.

[12] C. Mura, D. Cascio, M.R. Sawaya, D.S. Eisenberg, The crystal structure of a heptameric archaeal Sm protein: implications for the eukaryotic snRNP core, Proc. Natl. Acad. Sci. U.S.A. 98 (2011) 5532−5537, https://doi.org/10.1073/pnas.091102298.

[13] I. Törö, S. Thore, C. Mayer, J. Basquin, B. Séraphin, D. Suck, RNA binding in an Sm core domain: X-ray structure and functional analysis of an archaeal Sm protein complex, EMBO J. 20 (2001) 2293−2303, https://doi.org/10.1093/emboj/20.9.2293.

[14] S. Fischer, J. Benz, B. Späth, L.K. Maier, J. Straub, M. Granzow, M. Raabe, H. Urlaub, J. Hoffmann, B. Brutschy, T. Allers, J. Soppa, A. Marchfelder, The archaeal Lsm protein binds to small RNAs, J. Biol. Chem. 285 (45) (2010) 34429−34438, https://doi.org/10.1074/jbc.M110.118950.

[15] C. Mura, P.S. Randolph, J. Patterson, A.E. Cozen, Archaeal and eukaryotic ho-mologs of Hfq: a structural and evolutionary perspective on Sm function, RNA Biol. 10 (2013) 636−651, https://doi.org/10.4161/rna.24538.

[16] T.T. Kazimierz, G.K. Nikolay, K.C. Nicholas, F. Victor, J.A. Steitz, The ever-growing world of small nuclear ribonucleoproteins, in: The RNA World 3rd Edit, vol. 43, Cold Spring Harbor Monographs, 2006.

[17] J. Salgado-Garrido, E. Bragado-Nilsson, S. Kandels-Lewis, B. Séraphin, Sm and Sm-like proteins assemble in two related complexes of deep evolutionary origin, EMBO J. 18 (1999) 3451−3462, https://doi.org/10.1093/emboj/18.12.3451.

[18] M.T. Franze de Fernandez, L. Eoyang, J.T. August, Factor fraction required for the synthesis of bacteriophage Qbeta-RNA, Nature 10 (5154) (1968) 588−590, https://doi.org/10.1038/219588a0, 219.

[19] G.G. Carmichael, K. Weber, A. Niveleau, A.J. Wahba, The host factor required for RNA phage Qbeta RNA replication in vitro. Intracellular location, quanti-tation, and purification by polyadenylate-cellulose chromatography, J. Biol. Chem. 250 (1975) 3607−3612.

[20] D. Schuppli, G. Miranda, H.C. Tsui, M.E. Winkler, J.M. Sogo, H. Weber, Altered 3'-terminal RNA structure in phage Qbeta adapted to host factor-less *Escherichia coli*, Proc. Natl. Acad. Sci. U.S.A. 94 (1997) 10239−10242, https://doi.org/10.1073/pnas.94.19.10239.

[21] K.M. Wassarman, F. Repoila, C. Rosenow, G. Storz, S. Gottesman, Identification of novel small RNAs using comparative genomics and microarrays, Genes Dev. 15 (2001) 1637−1651, https://doi.org/10.1101/gad.901001.

[22] H.C. Tsui, H.C. Leung, M.E. Winkler, Characterization of broadly pleiotropic phenotypes caused by an Hfq insertion mutation in *Escherichia coli* K-12, Mol. Microbiol. 13 (1) (1994) 35−49, https://doi.org/10.1111/j.1365-2958.1994.tb00400.x.

[23] A. Zhang, S. Altuvia, A. Tiwari, L. Argaman, R. Hengge-Aronis, G. Storz, The OxyS regulatory RNA represses rpoS translation and binds the Hfq (HF-I) protein, EMBO J. 17 (1998) 6061−6068, https://doi.org/10.1093/emboj/17.20.606.

[24] D.D. Sledjeski, C. Whitman, A. Zhang, Hfq is necessary for regulation by the untranslated RNA DsrA, J. Bacteriol. 183 (2001) 1997−2005, https://doi.org/10.1128/JB.183.6.1997-2005.2001.

[25] T. Møller, T. Franch, C. Udesen, K. Gerdes, P. Valentin-Hansen, Spot 42 RNA mediates discoordinate expression of the *E. coli* galactose operon, Genes Dev. 16 (2002) 1696−1706, https://doi.org/10.1101/gad.231702.

[26] J.R. Chambers, K.S. Bender, The RNA chaperone Hfq is important for growth and stress tolerance in *Francisella novicida*, PloS One 6 (5) (2011), e19797, https://doi.org/10.1371/journal.pone.0019797.

[27] M.K. Chiang, M.C. Lu, L.C. Liu, C.T. Lin, Y.C. Lai, Impact of Hfq on global gene expression and virulence in *Klebsiella pneumoniae*, PloS One 6 (7) (2011), e22248, https://doi.org/10.1371/journal.pone.0022248.

[28] C.M. Brennan, M.L. Keane, T.M. Hunt, M.T. Goulet, N.Q. Mazzucca, Z. Sexton, T. Mezoian, K.E. Douglas, J.M. Osborn, B.J. Pellock, *Shewanella oneidensis* Hfq promotes exponential phase growth, stationary phase culture density, and cell survival, BMC Microbiol. 13 (2013) 33, https://doi.org/10.1186/1471-2180-13-33.

[29] J.L. Lai, D.J. Tang, Y.W. Liang, R. Zhang, Q. Chen, Z.P. Qin, Z.H. Ming, J.L.(Tang, The RNA chaperone Hfq is important for the virulence, motility and stress tolerance in the phytopathogen *Xanthomonas campestris*, Environ. Microbiol. Rep. 10 (5) (2018) 542—554, https://doi.org/10.1111/1758-2229.12657.

[30] H. Yao, M. Kang, Y. Wang, Y. Feng, S. Kong, X. Cai, Z. Ling, S. Chen, X. Jiao, Y. Yin, An essential role for Hfq involved in biofilm formation and virulence in serotype 4b *Listeria monocytogenes*, Microbiol. Res. 215 (2018) 148—154, https://doi.org/10.1016/j.micres.2018.07.001.

[31] J. Vogel, A rough guide to the non-coding RNA world of *Salmonella*, Mol. Microbiol. 71 (2009) 1—11, https://doi.org/10.1111/j.1365-2958.2008.06505.x.

[32] Y. Chao, J. Vogel, The role of Hfq in bacterial pathogens, Curr. Opin. Microbiol. 13 (2010) 24—33, https://doi.org/10.1016/j.mib.2010.1001.1001.

[33] S. Thore, C. Mayer, C. Sauter, S. Weeks, D. Suck, Crystal structures of the *Pyrococcus abyssi* Sm core and its complex with RNA: common features of RNA binding in Archaea and Eukarya, J. Biol. Chem. 278 (2003) 1239—1247, https://doi.org/10.1074/jbc.M207685200.

[34] B. Martens, G.A. Bezerra, M.J. Kreuter, I. Grishkovskaya, A. Manica, V. Arkhipova, K. Djinovic-Carugo, U. Bläsi, The Heptameric SmAP1 and SmAP2 proteins of the crenarchaeon *Sulfolobus solfataricus* bind to common and distinct RNA targets, Life 5 (2015) 1264—1281, https://doi.org/10.3390/life5021264.

[35] B. Martens, L. Hou, F. Amman, M.T. Wolfinger, E. Evguenieva-Hackenberg, U. Blasi, The SmAP1/2 proteins of the crenarchaeon *Sulfolobus solfataricus* interact with the exosome and stimulate A-rich tailing of transcripts, Nucleic Acids Res. 45 (2017) 7938—7949, https://doi.org/10.1093/nar/gkx437.

[36] L.K. Maier, J. Benz, S. Fischer, M. Alstetter, K. Jaschinski, R. Hilker, A. Becker, T. Allers, J. Soppa, A. Marchfelder, Deletion of the Sm1 encoding motif in the *lsm* gene results in distinct changes in the transcriptome and enhanced swarming activity of *Haloferax* cells, Biochimie 117 (2015) 129—137, https://doi.org/10.1016/j.biochi.2015.02.023.

[37] F. Rodriguez-Valera, G. Juez, D.J. Kushner, *Halobacterium mediterranei* spec, nov., a new carbohydrate-utilizing extreme halophile, Syst. Appl. Microbiol. 4 (3) (1983) 369—381, https://doi.org/10.1016/S0723-2020(83)80021-6.

[38] M.F. Mullakhanbhai, H. Larsen, *Halobacterium volcanii* spec. nov., a Dead Sea halobacterium with a moderate salt requirement, Arch. Microbiol. 104 (3) (1975) 207—214, https://doi.org/10.1007/BF00447326.

[39] P. López-García, A. St Jean, R. Amils, R.L. Charlebois, Genomic stability in the archaeae *Halobacterium volcanii* and *Haloferax mediterranei*, J. Bacteriol. 177 (5) (1995) 1405—1408, https://doi.org/10.1128/jb.177.5.1405-1408.1995.

[40] G. Payá, V. Bautista, M. Camacho, M.J. Bonete, J. Esclapez, New proposal of nitrogen metabolism regulation by small RNAs in the extreme halophilic archaeon *Haloferax mediterranei*, Mol. Genet. Genom. 295 (3) (2020) 775—785, https://doi.org/10.1007/s00438-020-01659-9.

[41] G. Payá, V. Bautista, M. Camacho, N. Castejón-Fernández, L.A. Alcaraz, M.J. Bonete, J. Esclapez, Small RNAs of *Haloferax mediterranei*: identification and potential involvement in nitrogen metabolism, Genes 9 (2) (2018) 83, https://doi.org/10.3390/genes9020083.

[42] S. Cai, L. Cai, H. Liu, X. Liu, J. Han, J. Zhou, H. Xiang, Identification of the haloarchaeal phasin (PhaP) that functions in polyhydroxyalkanoate accumulation and granule formation in *Haloferax mediterranei*, Appl. Environ. Microbiol. 78 (6) (2012) 1946—1952, https://doi.org/10.1128/AEM.07114-11.

[43] L. Pedro-Roig, C. Lange, M.J. Bonete, J. Soppa, J. Maupin-Furlow, Nitrogen regulation of protein-protein interactions and transcript levels of GlnK PII regulator and AmtB ammonium transporter homologs in Archaea, Microbiol. Open 2 (5) (2013) 826—840, https://doi.org/10.1002/mbo3.120.

[44] F. Rodríguez-Valera, F. Ruiz-Berraquero, A. Ramos-Cormezana, Behaviour of mixed populations of halophilic bacteria in continuous cultures, Can. J. Microbiol. 26 (1980) 1259—1263, https://doi.org/10.1139/m80-210.

[45] M. Hammelmann, J. Soppa, Optimized generation of vectors for the construction of *Haloferax volcanii* deletion mutants, J. Microbiol. Methods 75 (2) (2008) 201—204, https://doi.org/10.1016/j.mimet.2008.05.029.

[46] S.F. Altschul, W. Gish, W. Miller, E.W. Myers, D.J. Lipman, Basic local alignment search tool, J. Mol. Biol. 215 (1990) 403—410, https://doi.org/10.1016/S0022-2836(05)80360-2.

[47] K.L. Britto, P.J. Baker, M. Fisher, S. Ruzheinikov, D.J. Gilmour, M.J. Bonete, J. Ferrer, C. Pire, J. Esclapez, D.W. Rice, Analysis of protein solvent interactions in glucose dehydrogenase from the extreme halophile *Haloferax mediterranei*, Proc. Natl. Acad. Sci. U.S.A. 103 (13) (2006) 4846—4851, https://doi.org/10.1073/pnas.0508854103.

[48] E.A. Becker, P.M. Seitzer, A. Tritt, D. Larsen, M. Krusor, A.I. Yao, D. Wu, D. Madern, J.A. Eisen, A.E. Darling, M.T. Facciotti, Phylogenetically driven sequencing of extremely halophilic archaea reveals strategies for static and dynamic osmo-response, PLoS Genet. 10 (2014), e1004784, https://doi.org/10.1371/journal.pgen.1004784, 11.

[49] T. Achsel, H. Brahms, B. Kastner, A. Bachi, M. Wilm, R. Lührmann, A doughnut-shaped heteromer of human Sm-like proteins binds to the 3-prime end of U6 snRNA, thereby facilitating U4/U6 duplex formation *in vitro*, EMBO J. 18 (1999) 5789—5802, https://doi.org/10.1093/emboj/18.20.5789.

[50] E. Sauer, Structure and RNA-binding properties of the bacterial LSm protein Hfq, RNA Biol. 10 (4) (2013) 610—618, https://doi.org/10.4161/rna.24201.

[51] Y.I. Wolf, I.B. Rogozin, A.S. Kondrashov, E.V. Koonin, Genome alignment, evolution of prokaryotic genome organization, and prediction of gene function using genomic context, Genome Res. 11 (3) (2001) 356—372, https://doi.org/10.1101/gr.gr-1619r.

[52] E.V. Koonin, M.Y. Galperin, Sequence - Evolution - Function: Computational Approaches in Comparative Genomics, Kluwer Academic, Boston, 2003 (Chapter 5) Genome Annotation and Analysis, https://www.ncbi.nlm.nih.gov/books/NBK20253/.

[53] J. Caillet, B. Baron, I.V. Boni, C. Caillet-Saguy, E. Hajnsdorf, Identification of protein-protein and ribonucleoprotein complexes containing Hfq, Sci. Rep. 9 (2019) 1, https://doi.org/10.1038/s41598-019-50562-w.

[54] M. Kajitani, A. Kato, A. Wada, Y. Inokuchi, A.J. Ishihama, Regulation of the *Escherichia coli hfq* gene encoding the Host Factor for phage Q beta, Bacteriol 176 (2) (1994) 531—534.

[55] J.M. Andrade, R.F. Dos Santos, I. Chelysheva, Z. Ignatova, C.M. Arraiano, The RNA-binding protein Hfq is important for ribosome biogenesis and affects translation fidelity, EMBO J. 37 (2018), e97631, https://doi.org/10.15252/embj.201797631, 11.

[56] J. Esclapez, G. Bravo-Barrales, V. Bautista, C. Pire, M. Camacho, M.J. Bonete, Effects of nitrogen sources on the nitrate assimilation in *Haloferax mediterranei*: growth kinetics and transcriptomic analysis, FEMS Microbiol. Lett. 350 (2) (2014) 168—174, https://doi.org/10.1111/1574-6968.12325.

[57] K. Singh-Wissmann, J.G. Ferry, Transcriptional regulation of the phosphotransacetylase-encoding and acetate kinase-encoding genes (*pta* and *ack*) from *Methanosarcina thermophila*, J. Bacteriol. 177 (7) (1995) 1699—1702, https://doi.org/10.1128/jb.177.7.1699-1702.1995.

[58] E. Puerta-Fernández, A. Vioque, Hfq is required for optimal nitrate assimilation in the cyanobacterium *Anabaena* sp. Strain PCC 7120, J. Bacteriol. 193 (14) (2011) 3546—3555, https://doi.org/10.1128/JB.00254-11.

[59] E. Sonnleitner, S. Hagens, F. Rosenau, S. Wilhelm, A. Habel, K.E. Jäger, U. Bläsi, Reduced virulence of a *hfq* mutant of *Pseudomonas aeruginosa* O1, Microb. Pathog. 35 (5) (2003) 217—228, https://doi.org/10.1016/s0882-4010(03)00149-9.

[60] Y. Ding, B.M. Davis, M.K. Waldor, Hfq is essential for *Vibrio cholerae* virulence and downregulates σE expression, Mol. Biol. 53 (1) (2004) 345—354, https://doi.org/10.1111/j.1365-2958.2004.04142.x.

[61] A. Sittka, V. Pfeiffer, K. Tedin, J. Vogel, The RNA chaperone Hfq is essential for the virulence of *Salmonella typhimurium*, Mol. Microbiol. 63 (1) (2007) 193—217, https://doi.org/10.1111/j.1365-2958.2006.05489.x.

[62] D. Dienst, U. Dühring, H.J. Mollenkopf, J. Vogel, J. Golecki, W.R. Hess, A. Wilde, The cyanobacterial homologue of the RNA chaperone Hfq is essential for motility of *Synechocystis* sp. PCC 6803, Microbiology 154 (10) (2008) 3134—3143, https://doi.org/10.1099/mic.0.2008/020222-0.

[63] K. Jaschinski, J. Babski, M. Lehr, A. Burmester, J. Benz, R. Heyer, M. Dörr, A. Marchfelder, J. Soppa, Generation and phenotyping of a collection of sRNA gene deletion mutants of the haloarchaeon *Haloferax volcanii*, PLoS One 9 (3) (2014), e90763, https://doi.org/10.1371/journal.pone.0090763.

[64] M.K. Thomason, F. Fontaine, N. De Lay, G. Storz, A small RNA that regulates motility and biofilm formation in response to changes in nutrient availability in *Escherichia coli*, Mol. Microbiol. 84 (1) (2012) 17—35, https://doi.org/10.1111/j.1365-2958.2012.07965.x.